Chemical Engineering Journal 162 (2010) 557–564

Contents lists available at ScienceDirect

Chemical Engineering Journal

journal homepage: www.elsevier.com/locate/cej

The modelling of ozone mass transfer in static mixers using Back Flow Cell Model

Chedly Tizaoui [a,*], Yanmin Zhang [b]

[a] The Centre for Clean Water Technologies, School of Engineering, Swansea University, Singleton Park, Swansea SA2 8PP, United Kingdom
[b] Yorkshire Water Services, Western House, Halifax Road, Bradford BD6 2SZ, United Kingdom

ARTICLE INFO

Article history:
Received 19 April 2010
Received in revised form 27 May 2010
Accepted 27 May 2010

Keywords:
Back Flow Cell Model
Backmixing
Mass transfer
Ozone
Static mixer

ABSTRACT

Static mixers are efficient devices successfully used in water and wastewater treatment such as water ozonation for disinfection and oxidation. The growing interest in new ozone generators delivering high ozone concentrations at low gas flow rates has made static mixers an excellent choice for dissolving ozone into water. However it is still a challenging issue when there is a need to design static mixers for their best process performance. A modelling tool is then required to aid with static mixer design, especially for ozonation processes. In this study, Back Flow Cell Model (BFCM), which is a two-parameter model, was used to simulate at steady state ozone mass transfer from the gas phase to water in Kenics static mixer. Mass transfer resistance developed in the liquid phase controlled the process and was described by a volumetric mass transfer coefficient $k_l a$. The model parameters, number of cells (N) and back flow ratio (α), were determined from RTD tracer studies and did not change significantly with the gas-to-liquid volumetric flow rate ratios (Q_G/Q_L). The model was validated with experimental data and was found to be able to accurately predict the gas and liquid concentrations at the outlet of the mixer alongside ozone transfer efficiency. The BFCM was found reliable, accurate and simple to use. It also offers advantage of being flexible and simple to implement over other models and can be used for efficient static mixer design for ozonation processes.

1. Introduction

Ozone has gained over the past decades recognition of its beneficial applications in water and wastewater treatment due to its high disinfection and oxidation properties ($E^\circ = 2.07$ V at pH = 0) and generally does not generate harmful by-products as the case for chlorine, except bromate from bromide-containing waters [1,2] and in some rare cases trihalomethanes for example in waters containing algae [3,4]. Ozone is also advantageous in reducing costs to remove/avoid the by-products formed following water chlorination. In most cases, water treatment with ozone involves the use of gas/liquid contacting devices to transfer ozone, which is produced on-site in pure oxygen or air, to the water. Examples of these gas/liquid contactors include bubble columns, static mixers, diffusers, injectors and deep U tube. Static mixers are of particular interest due to the many advantages that they offer as compared to other gas/liquid contacting devices and as such they are successfully applied in water and wastewater treatment processes for both chemical oxidation and disinfection [5–12]. In comparison to fine bubble columns (FBC), which are the conventional gas/liquid contactors used in the water industry, static mixers achieve high ozone mass transfer efficiencies (>95% and in some cases can almost reach 100% as compared to <92% in FBC) [13,14]. Moreover, for a similar performance, the size of a static mixer is much smaller than the size of a bubble column. Therefore less space is required for installation, which leads to reduction in capital costs. Static mixers can be mounted either horizontally or vertically and present no moving parts thus requiring almost no maintenance.

Over two decades ago, requirements to minimise the costs of ozone generation led to the development of new medium frequency ozone generators that deliver high ozone concentrations but involve low gas flow rates. At low gas flow rates, the gas-to-liquid volumetric flow rates ratio (Q_G/Q_L) is also low, hence conventional fine bubble diffusion columns are not adequate anymore. This is because a sufficient gas flow rate to ensure adequate gas/liquid mixing, hence adequate ozone transfer, is required in FBC. In fact, when bubble columns are used, low Q_G/Q_L ratio poses problems in the gas flow hydrodynamics causing for example channelling which reduces the performance of the contactor. Although in FBC, supplement gas can be provided to the main low flow rate ozone gas stream in order to avoid the hydrodynamic problems, the performance of the ozonation system may be jeopardised as a result of ozone concentration reduction due to gas dilution. Static mixers overcome these problems and in fact are more efficient at low Q_G/Q_L ratios and high feed gas ozone concentrations [14]. Complete benefit from the high ozone concentration generated by modern medium frequency ozone generators is therefore

* Corresponding author. Tel.: +44 0 1792 295587; fax: +44 0 1792 295676.
E-mail addresses: c.tizaoui@swansea.ac.uk, chedly.tizaoui@nottingham.ac.uk (C. Tizaoui).

1385-8947/$ – see front matter © 2010 Elsevier B.V. All rights reserved.
doi:10.1016/j.cej.2010.05.061

gained when static mixers are used. For these reasons, static mixers have been increasingly used to enhance ozone transfer in water [6,9,15,16]. A maximum design gas-to-liquid volumetric flow rate ratio (Q_G/Q_L) value of 0.5 $m^3\,s^{-1}/m^3\,s^{-1}$ has been suggested in the literature.

Static mixers are capable to ensure homogenous ozone concentrations due to internal high turbulence created by the mixer elements, which ensures high mixing between the gas and the liquid. The flow of both phases may approach piston for high mixer lengths and the mixing is intensive in the radial direction. Uniform distribution of small bubbles over the whole mixer is obtained resulting in high interfacial area and high mass transfer rates. However, the specific power consumption can be high due to high pressure drop that develops in the mixer. The behaviour of the flow inside static mixers is generally complex and involves islands or pockets, is three-dimensional and spatially periodic in the axial direction particularly in the case of Kinecs mixers [17–20]. Jones et al. [21] have demonstrated numerically the presence of pockets of reversed flow and strong longitudinal vortices in helical static mixers and Nauman et al. [20] have developed a static mixer that promotes axial mixing. Hobbs and Muzzio [17] have shown that the performance of the mixer depends largely on the mixer Reynolds number (Re) values and found that it performs well for creeping flow conditions ($Re \leq 10$).

Clearly, the hydrodynamics that develop in the static mixer during the flow of gas–liquid systems are complex and have great influence on the overall mass transfer performance of the mixer. As a result it is still challenging to design static mixers for their best process performance. A modelling tool is therefore needed to aid with such a task, especially for ozonation processes. Although Back Flow Cell Model (BFCM) is a flexible and accurate modelling technique dating back to the 1960s, it was not explored for the modelling of ozone mass transfer in static mixers, hence this study was carried out.

2. Model development

2.1. Back Flow Cell Model (BFCM)

BFCM is an improvement to the ordinary tanks-in-series model (TSM). In fact TSM does not take into account of upstream mixing of material but this limitation was avoided by the introduction of back flow between the cells in BFCM. The back flow ratio, α, constitutes the main parameter in BFCM. Depending on values of this ratio, the performance of the model changes between that of a single stirred tank ($\alpha \to \infty$) and an ordinary tanks-in-series ($\alpha \to 0$). It is evident that BFCM and the classical axial dispersion model (ADM) are related, because both of them take into account of the same phenomenon, though they represent it differently. Indeed for a given value of α, BFCM converges to the ADM as the number of cells increases. However, BFCM is wider in its application and covers a variety of systems ranging from stagewise to axial mixing (i.e. dispersion) continuous processes. An approximate relationship between the parameters of both models may be given by Eq. (1). The terms 0.5 and α refer to the perfect mixing in each cell and the backmixing between cells respectively. The total backmixing is the sum of these two effects and represented by N/Pe.

$$\frac{N}{Pe} = \alpha + 0.5 \tag{1}$$

Roemer and Durbin [22] have proposed for BFCM, analytical expressions for the dimensionless residence time distribution (RTD) function, E_θ, and the normalised variance, σ_θ^2:

$$E_\theta = \sum_{i=1}^{N} [A_i \exp(s_i \theta)] \tag{2}$$

$$\sigma_\theta^2 = \frac{1+\alpha}{N^2}[(N+\alpha)(1+\lambda) + \alpha(1+2\lambda^N) - 4(1+\alpha)\lambda - (1+\alpha)\lambda^2] \tag{3}$$

where $\alpha = Q_B/Q$; $\lambda = \alpha/(1+\alpha)$; Q: feed flow rate; Q_B: back flow rate; N: number of cells

$$A_i = (-2N\lambda^{-N/2}) \left(\frac{\sin^2(\varphi_i)}{D'(\varphi_i)} \right);$$

$$s_i = \left(\frac{N}{1-\lambda} \right) [2\lambda^{0.5} \cos(\varphi_i) - (1+\lambda)]$$

$D'(\varphi_i)$ is the derivative at the point φ_i of the function: $D(\varphi) = \lambda^{-0.5} \sin((N+1)\varphi) - 2\sin(N\varphi) + \lambda^{0.5} \sin((N-1)\varphi)$; and φ_i are the roots of the equation $D(\varphi) = 0$ in the interval $0 < \varphi_i < \pi$.

The above equations were implemented in Matlab Version R2009 and fitted to experimental data obtained from pulse injection test by minimising the square error function (Eq. (4)) with respect to the parameters N and α:

$$e_p(N, \alpha) = \sum_{i=1}^{n_p} [E_\theta(\theta_i, N, \alpha) - E_{\theta i}]^2 \tag{4}$$

where E_θ is the value of the dimensionless RTD function at the normalised time θ_i calculated by Eq. (2), and $E_{\theta i}$ is the experimental value.

2.2. BFCM for ozone mass transfer in the static mixer

A BFCM model was developed to predict ozone mass transfer in a Kenics static mixer. A schematic representation of this model for upward co-current flow is shown in Fig. 1. In order to characterise backmixing in the liquid phase, the model assumes a fraction α of the entrance liquid flow rate is returned from an upper cell to the nearest lower cell (back flow) and in return the same fraction is exchanged from the lower cell to the upper cell (exchange flow). Backmixing in the gas phase is assumed negligible [23]. Each phase is represented by a series of N cells and each cell is assumed being completely mixed. Mass transfer is assumed to take place at the interface between adjacent cells at a rate described by a constant volumetric mass transfer coefficient, $k_l a$. It is also assumed that the number of cells in each phase is the same so mass transfer can easily be described as occurring between neighbouring cells (Fig. 1). In Fig. 1, the dotted cells (0 and $N+1$) represent virtual cells with negligible hold-up and volume so flow exchanges (i.e. backmixing) at the boundaries of the mixer can easily be taken into account.

Further assumptions used in the development of the model are:

- the system is operated under steady state conditions;
- dilute system;
- liquid and gas flow rates are constant along the mixer length;
- mass transfer resistance for ozone absorption is confined to the liquid side alone because ozone is sparingly soluble in water;
- gas hold-up and interfacial area are constant along the mixer length;
- the rate of ozone decay is pseudo-first-order in the liquid phase, and is negligible in the gas phase;
- Henry's law applies for ozone equilibrium concentration in water.

On the basis of these assumptions, ozone mass transfer in the static mixer was described by the following system of algebraic

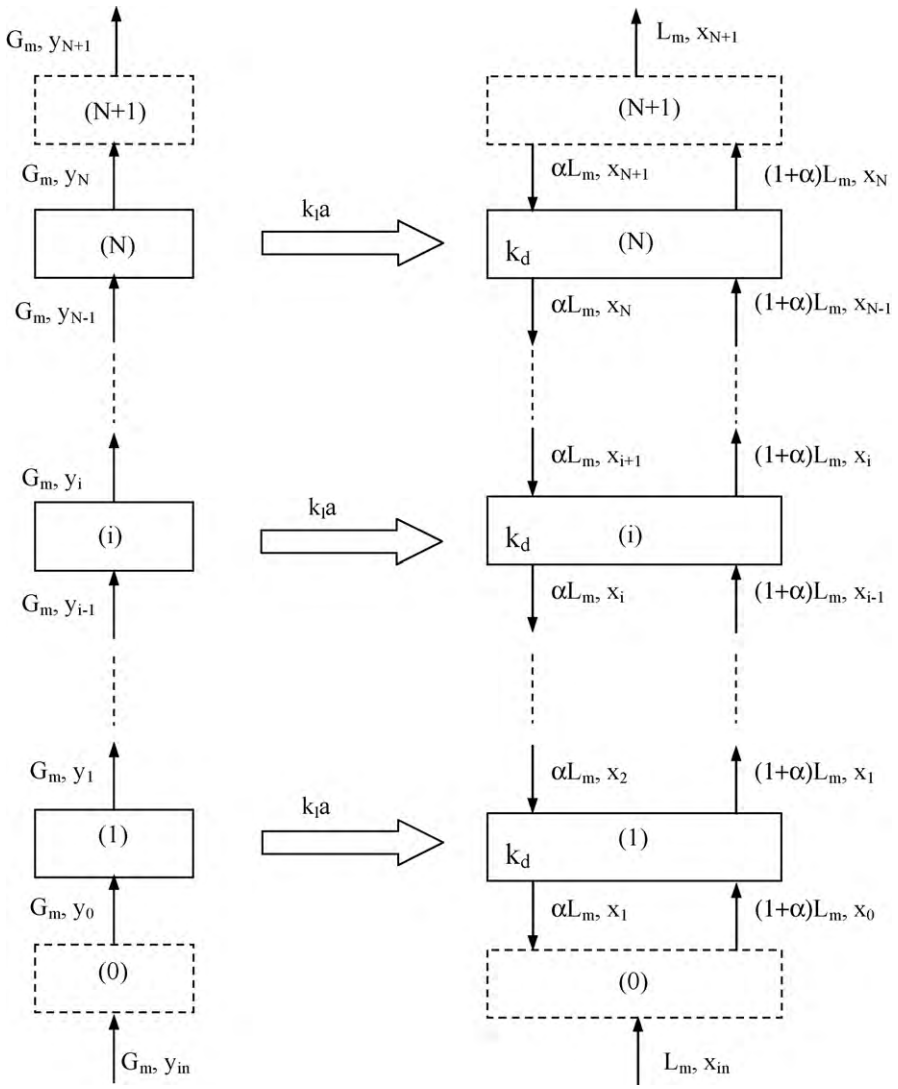

Fig. 1. Schematic representation of the BFCM (L_m: molar liquid flow rate (mol/s); G_m: molar gas flow rate (mol/s); x: ozone molar fraction in liquid phase; y: ozone molar fraction in gas phase; i: cell number; k_d: first-order ozone decay rate constant (s^{-1}); α: back flow ratio; N: total number of cells).

equations. These equations are the result of mass balances relative to ozone in the gas and liquid phases around a cell i (Fig. 1).

(i) gas phase

$$i = 0 \quad y_0 = y_{\text{in}} \tag{5}$$

$$1 \le i \le N \quad y_{i-1} - y_i + b_4 x_i - b_4 x_i^* = 0 \tag{6}$$

$$i = N+1 \quad y_{N+1} = y_{\text{out}} = y_N \tag{7}$$

(ii) liquid phase

$$i = 0 \quad x_0 = \frac{b_2 x_1 - x_{\text{in}}}{b_0} \tag{8}$$

$$i = 1 \quad (b_2 - b_1)x_1 + b_2 x_2 + b_3 x_1^* = x_{\text{in}} \tag{9}$$

$$2 \le i \le N \quad b_0 x_{i-1} - b_1 x_i + b_2 x_{i+1} + b_3 x_i^* = 0 \tag{10}$$

$$i = N+1 \quad x_{N+1} = x_{\text{out}} = x_N \tag{11}$$

where $b_0 = 1 + \alpha$; $b_1 = 1 + 2\alpha + (k_l a + k_d)\frac{V_c}{L}$; $b_2 = \alpha$;

$b_3 = k_l a \frac{V_c}{L}$; $b_4 = k_l a \frac{V_c}{G}$

$k_l a$ is the volumetric mass transfer coefficient; V_c is the volume of a liquid cell calculated as the total liquid volume divided by N; k_d is the first-order rate constant for ozone decay in water calculated by [24]:

$$k_d = 5.43 \times 10^3 \exp\left(-\frac{4964}{T}\right) \tag{12}$$

where k_d in s^{-1} and T in K.

x_i^* was calculated applying a modified Henry's law: $x_i^* = y_i/m$, where $m = H/P_T$; H is Henry's law constant given by Eq. (13) as function of temperature and pH [25]; and P_T is the total pressure in atm assumed constant.

$$H(\text{atm/mol/mol}) = 3.84 \times 10^7 (10^{\text{pH}-14})^{0.035} \exp\left(-\frac{2428}{T}\right) \tag{13}$$

The above mass balance equations can be easily written in a matrix form as below:

$$\begin{cases} [ML]\bar{x} + b_3\bar{x}^* = \bar{B}_L \\ [MG]\bar{y} + b_4\bar{x} - b_4\bar{x}^* = \bar{B}_G \\ \bar{x}^* = \dfrac{1}{m}\bar{y} \end{cases} \tag{14}$$

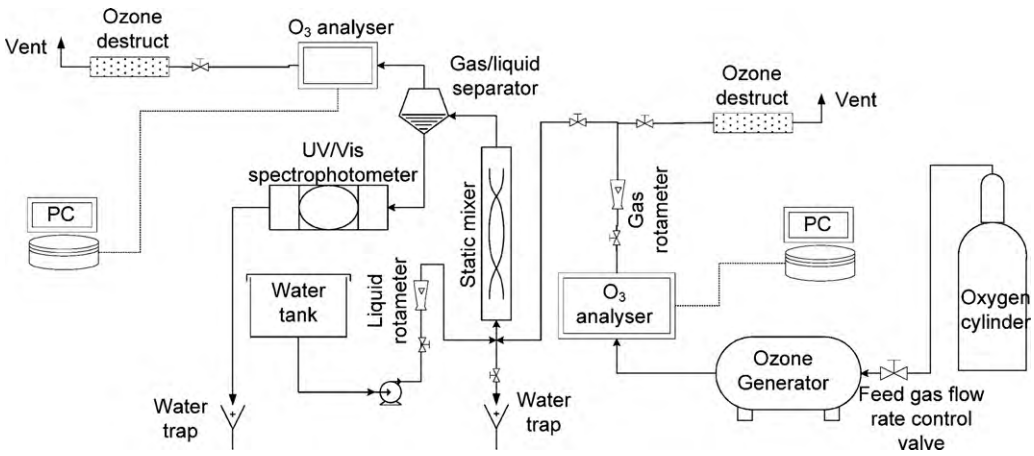

Fig. 2. Experimental set up.

where the matrices [*ML*] and [*MG*], and the vectors $\bar{x}$, $\bar{y}$, $\bar{x}^*$, $\bar{B}_L$ and $\bar{B}_G$, are defined by:

$$ML(1,1) = ML(N,N) = b_2 - b_1$$
$$2 \le i \le N-1,\ j \ne i-1, i, i+1: \quad ML(i,i) = -b_1; \quad ML(i,i-1) = b_0; \quad ML(i,i+1) = b_2; \quad ML(i,j) = 0$$
$$BL(1) = x_{in}$$
$$2 \le i \le N: \quad BL(i) = 0$$
$$MG(1,1) = -1$$
$$2 \le i \le N,\ j \ne i-1, i: \quad MG(i,i) = -1; \quad MG(i,i-1) = 1; \quad MG(i,j) = 0$$
$$BG(1) = -y_{in}$$
$$2 \le i \le N: \quad BG(i) = 0$$
$$1 \le i \le N: \quad x(i) = x_i; \quad y(i) = y_i; \quad x^*(i) = x_i^*$$

The above system of equations was then solved and lead to:

$$\bar{y} = [M]^{-1}\bar{B} \tag{15}$$

$$\bar{x} = [ML]^{-1}\bar{B}_L - \frac{b_3}{m}[ML]^{-1}[M]^{-1}\bar{B} \tag{16}$$

$$\bar{x}^* = \frac{1}{m}[M]^{-1}\bar{B} \tag{17}$$

where

$$[M] = [MG] - \frac{b_3 b_4}{m}[ML]^{-1} - \frac{b_4}{m}[I]$$

$$\bar{B} = \bar{B}_G - b_4[ML]^{-1}[B_L]$$

$[ML]^{-1}$ is the inverse of the matrix [*ML*] and [*I*] is the identity matrix.

All matrix calculations were carried out using Matlab Version R2009.

3. Materials and methods

Two assemblies of the same static mixer were used; both designed for laboratory tests. The first was designed to carry out residence time distribution experiments using a red dye (C.I. 147) as a tracer, and the second to study ozone mass transfer. The static mixer was a stainless steel Kenics type mixer fitted in a glass tube. It has an aspect ratio of 1.5, internal diameter 19.05 mm, and thickness of the helical strip 1.4 mm. Two lengths of this mixer were used, 37 cm (12 left- and right-hand helical elements) and 74 cm (24 left- and right-hand helical elements). In each case, the mixer was positioned vertically.

The experimental set up used in this study is shown in Fig. 2. Ozone was produced from pure oxygen using a small air-cooled plate ozone generator (BMT 803, BMT Messtechnik, Germany). Its gas concentration was measured using a dual beam UV photometer ozone analyser (BMT 963, BMT Messtechnik, Germany), which measures the ozone concentration in gram of ozone/m^3 of gas at normal conditions (NTP: 0 °C, 1atm) in the range 0–100 g/m^3 NTP. It was fitted with an isolated serial interface RS-232 connected to a computer for data acquisition. Gas flow rate varied between 400 and 800 mL/min and gas ozone concentration varied in the range 60–90 g/m^3 NTP. The liquid flow rate varied in the range 1.5–2.3 L/min. A Hewlett Packard 8451A Diode Array spectrophotometer was used to measure either dye concentrations for RTD experiments (λ_{max} = 540 nm) or dissolved ozone in water (λ_{max} = 260 nm). The water and gas flow rates were measured and controlled using throttle needle valve Platon flow meters. Since ozone is a very strong oxidant, high corrosion resistant materials were used for all components of the ozone system, including instruments, piping and fittings. Polytetrafluoroethylene (PTFE) was used for tubes and fittings carrying ozone-containing gas. Ozone in oxygen was introduced continuously into the mixer from the bottom co-currently with the liquid. RTD experiments were also carried out using the same experimental set up operated at various liquid and gas flow rates. Simultaneously with the tracer injection of a 100 mg/L solution of the dye at the inlet of the static mixer, the concentration of the tracer dye was measured at regular intervals of time (2 s) at the outlet of the mixer using the UV/VIS spectrophotometer (λ_{max} = 540 nm) until all the injected dye was recovered. Each experiment set was repeated three times. The gas used in the RTD experiments was ozone-free pure oxygen. No ozone was present in the gas stream because O_3 is reactive with the tracer dye. The reactivity of the dye with pure oxygen was checked and no reactivity was found.

4. Results and discussions

4.1. Tracer studies

The pulse tracer method, assumed ideal and being represented by a Dirac δ function, was used to study the liquid phase disper-

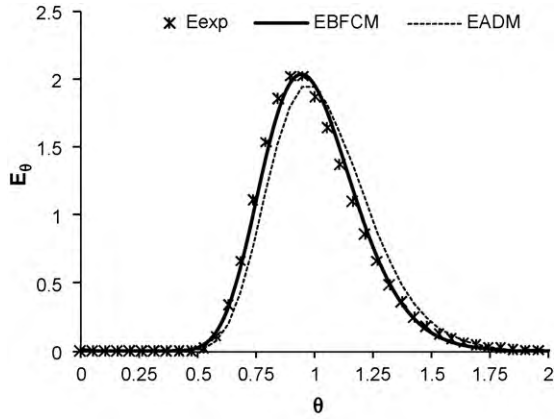

Fig. 3. Fittings of experimental results with BFCM (N = 39, α = 0.33) and ADM (Pe = 48) models; Q_G/Q_L = 0.8.

sion in the mixer using different values of the ratio Q_G/Q_L. The experimental response curves to the pulse input signal were then fitted using the BFCM and ADM models. The model parameters were determined by non-linear regression method. In the case of ADM only one parameter was determined (Pe) and in the case of BFCM two parameters were determined (α and N). A typical result is shown in Fig. 3 for a Q_G/Q_L = 0.8. Similar trends were also obtained for the other Q_G/Q_L ratios. Clearly, Fig. 3 shows that the BFCM gives better fit of the experimental results than that of ADM. It was found that the errors between model predictions and observed data were <5 and <13% for BFCM and ADM models respectively. This clearly indicates that BFCM was more accurate than ADM. This is indeed expected since BFCM depends on two parameters as compared to ADM which depends on only one parameter, so BFCM is more flexible in fitting the experimental results. Moreover, BFCM presents computational advantages since it deals with algebraic equations instead of differential equations. Fig. 3 also shows that BFCM modelled the tail of the RTD curve more accurately than ADM. In their study, Degaleesan et al. [26] also obtained that ADM was not accurate to model the tail of the RTD curve obtained from their bubble column study and they did not recommend using ADM to model their system. It is clear that BFCM, which depends on two parameters, is more powerful than ADM, which depends on only one parameter. Hence, in this study, BFCM was adopted for the modelling of ozone mass transfer in the static mixer.

The effect of Q_G/Q_L ratio on the number of cells, N and the backflow ratio, α, was studied. Fig. 4 shows that increasing the gas-to-liquid volumetric flow rates ratio did not affect significantly neither N nor α. This indicates that backmixing is not largely affected by the co-existence of the two phases under the experimental conditions used in this study. The average value of N was 38 ± 1 and that of α was 0.33 ± 0.01. Since it is general that static mixers are operated at ratios of Q_G/Q_L falling within the range covered in Fig. 4, the application of BFCM to model these gas/liquid contactors is plausible because a change in the liquid or gas flow rate will not affect the values of N and α, which can be determined for only one set of given gas and liquid flow rates.

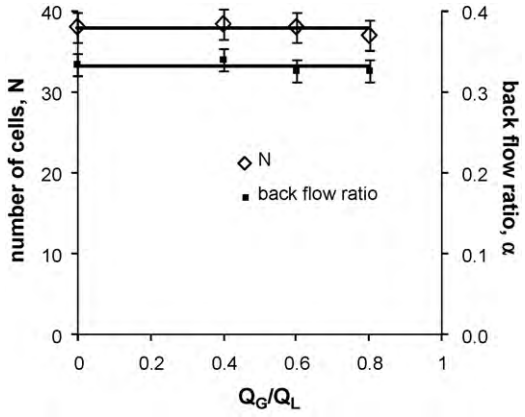

Fig. 4. Effect of the ratio Q_G/Q_L on the number of cells and back flow ratio of the BFCM model.

4.2. Volumetric mass transfer coefficient, k_la

An important parameter to characterise ozone mass transfer in static mixers is the mass transfer coefficient K_La, which sums up the influence of process parameters (e.g. flow rates, energy input) and physical parameters (e.g. density, viscosity, and surface tension) as well as reactor geometry. Ozone is sparingly soluble in water, therefore mass transfer rate is liquid film controlled and the overall volumetric mass transfer coefficient K_La is equivalent to that based on the individual liquid film, k_la. There are only few correlations in the literature describing gas-liquid mass transfer in some specific types of static mixers. Masschelein [24] has proposed an experimental correlation for K_L in bubble-generating systems of the form: $K_L = 1.13((D_{O3} \times v_R)/d_B)$ where D_{O3} is ozone diffusivity, v_R is the relative velocity of gas to water and d_B is the average bubble diameter. However the determination of d_B is very difficult. Heyouni et al. [27] have developed empirical equations to predict mass transfer coefficient and gas bubble diameter in three types of static mixers and they found that bubble size increases with gas flow rate whilst it decreases with liquid flow rate. Other models could be applied in static mixers including those used for bubbles in free ascension but these models do not take into account of bubble deformations along the static mixer. It is evident that appropriate correlation to determine mass transfer coefficient applicable to our system is difficult to obtain. Thus an experimental determination of the volumetric mass transfer k_la was adopted in this study.

Determination of mass transfer coefficient may be made through either unsteady state methods or through steady state methods. A steady state method was used in this work. It is based on solute (i.e. ozone) mass balance over the liquid phase, which led to Eq. (18). In this equation, changes in k_la due to mass transfer enhancement through ozone decay were neglected [28]. To take into account of the changes in the value of the driving force over the length of the static mixer, logarithmic concentration difference ΔC_{lm} was used (Eq. (19)).

$$k_la = \frac{Q_L}{V_L}\frac{C_L - C_{L0}}{\Delta C_{lm}} \tag{18}$$

$$\Delta C_{lm} = \frac{(C_{L0}^* - C_{L0}) - (C_L^* - C_L)}{\mathrm{Ln}((C_{L0}^* - C_{L0})/(C_L^* - C_L))} \tag{19}$$

where C_{L0}*: inlet liquid equilibrium concentration; C_L*: outlet liquid equilibrium concentration; C_{L0}: inlet liquid concentration; C_L: outlet liquid concentration.

Over the range of liquid and gas flow rates used in this study, k_la values varied between 0.1 and 0.3 s^{-1}; these values are typical for static mixers [27]. An empirical correlation to calculate k_la (s^{-1}) as function of liquid and gas velocities (m/s) based on empty tube was determined from the experimental data (Eq. (20)). A similar correlation was also proposed by Martin and Galey [9]. The relationship between experimental and calculated values of k_la is shown in Fig. 5, which indicates good agreement between the results.

$$k_la = 59.1u_L^{0.83}u_G^{1.14} \tag{20}$$

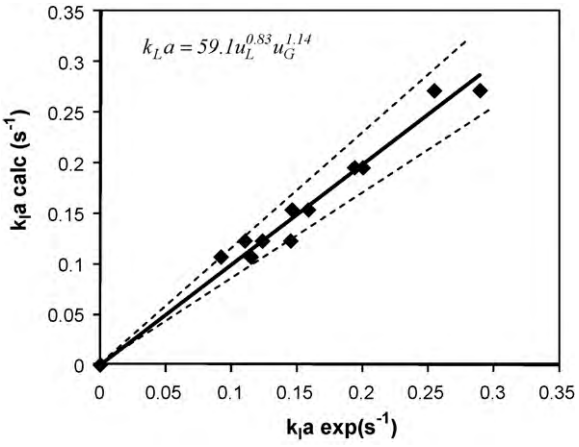

Fig. 5. Correlation of k_la values (Q_L = 1.5, 1.8, and 2.3 L/min; Q_G = 0.4, 0.6, and 0.8 L/min; C_{O3in} = 64 g/m^3 NTP; h = 37 and 74 cm; T = 20 °C).

4.3. Ozone mass transfer BFCM model validation

The validation of the developed model was carried out by comparing the output of the model to the experimental data. Two different lengths of the mixer (0.37 and 0.74 m) were used. The experiments were carried out at different flow rates of gas (400, 600, 800 mL/min) and liquid (1.5, 1.8, 2.3 L/min) and different inlet ozone gas concentrations (64 and 82 g/m^3 NTP). The model was run using the same operating conditions used in the experimental study. The results are plotted in Fig. 6 in the form of model outputs (i.e. x/x_{in}^* and y/y_{in}) as function of the obtained experimental values. The slopes of the lines giving the changes of gas phase composition and liquid phase composition obtained by the model and those obtained by experiments approach 1 with an error of ±7%. This clearly indicates good agreement between the model and experimental results, which validate the model for the range of operating conditions used.

The slight overestimation of the gas composition (+7%) or the slight underestimation of the liquid composition (−7%) at the outlet of the mixer by the model may due to errors as a result of inaccurate values of the ozone decay rate constant, k_d and/or ozone equilibrium concentration. In fact the rate of ozone decay depends on the type of water and experimental procedures used for measuring it. This resulted in many differing models presented in the literature and no single accurate model can be used for all types of waters [29] and the same applies for equilibrium concentration models.

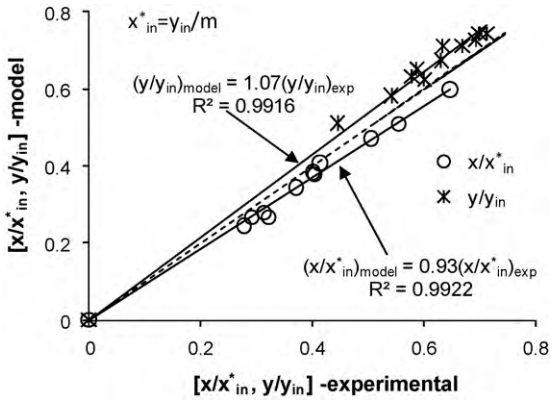

Fig. 6. Correlation between experimental and model results (Q_L = 1.5, 1.8, and 2.3 L/min; Q_G = 0.4, 0.6, and 0.8 L/min; C_{O3in} = 64 and 82 g/m^3 NTP; h = 37 and 74 cm; T = 20 °C).

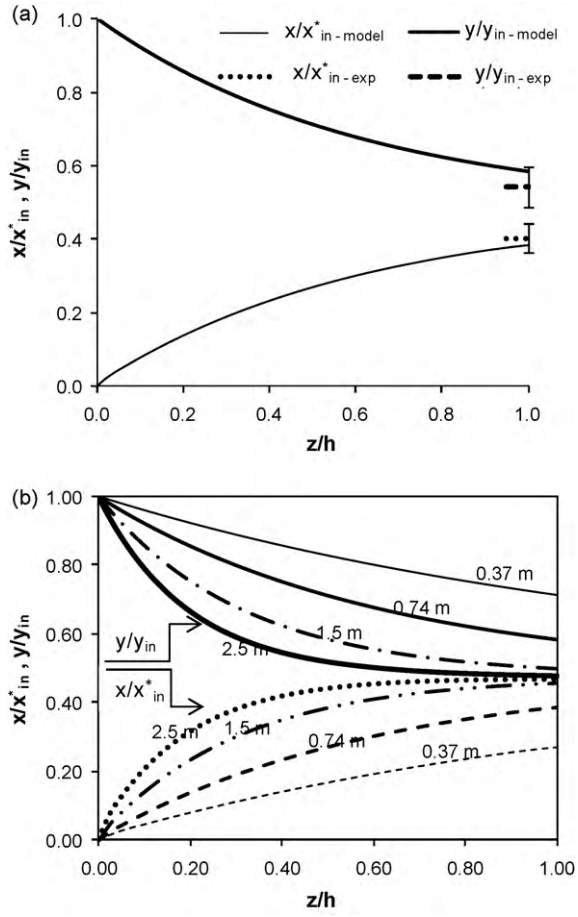

Fig. 7. Effect of mixer length on the profiles of gas and liquid compositions (Q_G = 0.4 L/min, Q_L = 1.8 L/min, C_{O3in} = 64 g/m^3 NTP) (a) mixer length h = 0.74 m, dashed lines for experimental results and continuous lines for model outputs; (b) different simulation total mixer lengths h.

4.4. Concentration profile along the length of the mixer

Estimation of the profile of gas and liquid concentrations along the length of the mixer was made. Typical profile is shown in Fig. 7(a) for a mixer total length of 0.74 m and gas-to-liquid volumetric flow rates ratio of 0.22. Clearly ozone concentration in the gas phase decreases along the length of the mixer while, as expected, the liquid concentration increases. At the outlet of the mixer (i.e. z/h = 1), the concentrations reach certain values away from equilibrium (i.e. $x/x_{in}^* \neq y/y_{in}$). This is due to insufficient contact time between the two phases. Fig. 7(a) also shows that at the outlet of the mixer (i.e. z/h = 1) the model predicts well the measured experimental values (shown by the dashed short lines), which again validates the model. The model was also run to simulate the changes of the profiles of ozone concentrations as function of the total length of the mixer so approach to equilibrium can be studied; the results are shown in Fig. 7(b). Increasing the length of the mixer resulted in continuously reducing the gas concentration along the length of the mixer while continuously increasing the liquid concentration leading to the gas and liquid curves approaching each other (i.e. approaching equilibrium). The figure also shows that a maximum possible liquid concentration (i.e. approach to equilibrium) can be achieved in a mixer having a length of about 2.5 m. Theoretically, equilibrium condition at the outlet of the mixer can only be achieved in a mixer having an infinite length, but an increase of the mixer length beyond about 2.5 m will not be advantageous in terms of mass transfer.

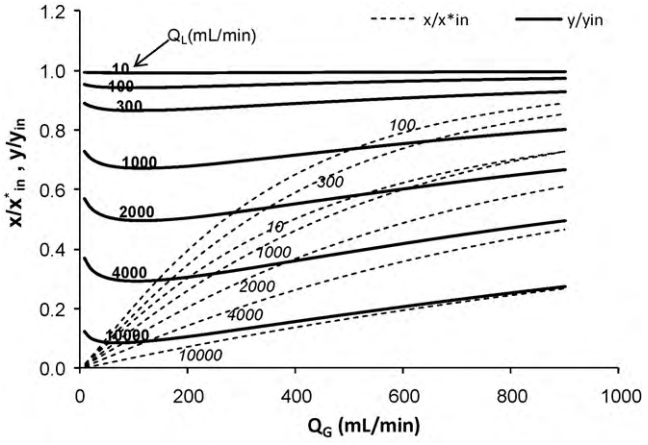

Fig. 8. Effect of gas and liquid flow rates on the exit gas and liquid concentrations (h = 0.74 m, pH = 7, T = 20 °C, C_{O3in} = 64 g/m^3 NTP).

4.5. Effect of gas and liquid flow rates on ozone mass transfer

The effect of gas and liquid flow rates on gas and liquid concentrations at the outlet of the mixer was studied and the results are shown in Fig. 8. The figure shows that for a given liquid flow rate, the exit liquid concentration (i.e. x/x_{in}^*) is more sensitive to changes in gas flow rate than does the gas concentration (i.e. y/y_{in}). The figure also shows that, the gas concentration decreases slightly by increasing the gas flow rate until reaching a minimum and further increase in the gas flow rate results in slow increase of the gas concentration. This trend is sustained for all liquid flow rates. However, the liquid concentration increases more rapidly following an increase in the gas flow rate due to the increase in the ratio Q_G/Q_L. Moreover, Fig. 8 shows that for a given gas flow rate, increasing the liquid flow rate leads to a maximum liquid concentration being reached after which further increase in liquid flow rate causes reduction in liquid concentrations. This can be explained by a trade off between enhancement of mass transfer as a result of an increase in the liquid flow rate (Eq. (20)) and a reduction of the ratio Q_G/Q_L coupled with increasing ozone decomposition rates as a result of increased liquid concentration.

To clearly illustrate the effect of water flow rate and the ratio Q_G/Q_L on the exit liquid and gas concentrations over a wide range of flow rates, three-dimensional plots are used (Fig. 9(a) and (b)). The simulations were made at a constant inlet ozone gas concentration of 64 g/m^3 NTP and a constant mixer length of 0.74 m. The shape of a "stool" shown in Fig. 9(a) represents the variation of the relative exit liquid concentration as function of liquid flow rate and the ratio Q_G/Q_L. The figure shows that for a given liquid flow rate lower than approximately 500 mL/min, the exit liquid ozone concentration increases with increasing the ratio Q_G/Q_L up to a maximum that depends on the value of the liquid flow rate. Nevertheless, when the liquid flow rate increases beyond approximately 500 mL/min, the maximum exit concentration becomes almost independent of the liquid flow rate at high Q_G/Q_L ratios. This indicates that to obtain the highest ozone liquid concentration at the exit of the mixer, not only the ratio Q_G/Q_L that should be carefully selected but in addition the liquid flow rate should also be chosen carefully. On the other hand for a given ratio Q_G/Q_L, the exit liquid concentration increases with increasing Q_L up to a maximum, which becomes independent of Q_G/Q_L for ratios higher than approximately 0.8. The region forming the top front edges of the "stool" obtained by the intersection between higher Q_L and higher Q_G/Q_L regions gives a plausible working region where the exit ozone concentration reaches its maximum. Because the static mixer is operated in co-current mode,

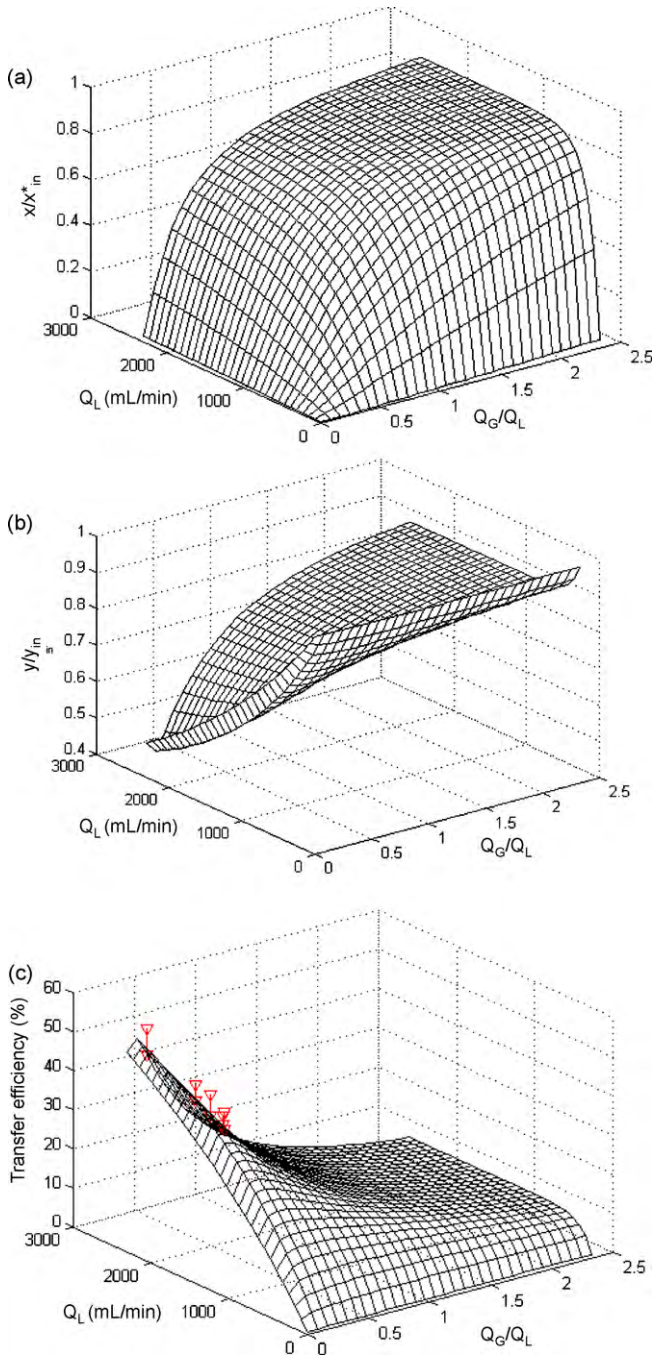

Fig. 9. 3-D plots of the effect of liquid and gas-to-liquid volumetric flow rates ratio on the exit gas and liquid concentrations and transfer efficiency (h = 0.74 m, C_{O3in} = 64 g/m^3 NTP, pH = 7, T = 20 °C).

the maximum exit liquid concentration will be determined by the equilibrium condition and the ratio x/x_{in}^* will always be less than 1.

Since most of the energy provided in an ozonation system is used for ozone generation hence a loss of ozone in the off-gas is not economical; consideration of the transfer efficiency is therefore very important. Fig. 9(b) and (c) shows the variation of the exit relative gas concentration and of ozone transfer efficiency (Eq. (21)) respectively as function of Q_L and the ratio Q_G/Q_L. The exit gas concentration (Fig. 9(b)) is minimum in the region of high liquid flow rate and low gas-to-liquid volumetric flow rate ratios. However it reaches maximum values in the region of low Q_L or high ratios Q_G/Q_L. This is reflected in the transfer efficiency (Fig. 9(c)) being

poor in the region of low liquid flow rates or high ratios Q_G/Q_L. The highest ozone transfer efficiency is obtained for the highest liquid flow rates but low ratios Q_G/Q_L. This agrees well with the fact that static mixers are generally operated at low Q_G/Q_L ratios (~0.5) in order to achieve high transfer efficiency. The maximum transfer efficiency achieved under the conditions used in this study was just below 50%. This ozone transfer efficiency can be improved (i.e. >95%) if either or both the length of the mixer and the liquid flow rate are increased. Experimental points with error bars are also shown in Fig. 9(c). Clearly good agreement was obtained between the transfer efficiencies calculated by the model and those obtained from the experiments with a relative error evaluated at about 12%.

$$\mathrm{TE} = 100 \times \frac{\text{transferred ozone}}{\text{inlet ozone}} \quad (21)$$

5. Conclusions

The ozone mass transfer in a Kenics static mixer was studied. A two-parameter Back Flow Cell Model was used to simulate ozone mass transfer in the mixer. The model parameters, number of cells (N) and back flow ratio (α), were determined from RTD tracer studies. It was found that N and α did not change significantly with the gas-to-liquid volumetric flow rates ratio (Q_G/Q_L). The parameters N and α were then used for ozone mass transfer simulations. The model was validated with experimental data and was used to simulate the effect of the operating parameters on the performance of the mixer. The profiles of ozone gas and liquid concentrations along the length of the mixer were determined. 3-D plots were used to ascertain the effect of Q_G/Q_L and Q_L on the liquid and gas ozone concentrations in addition to ozone transfer efficiency at the outlet of the mixer. High transfer efficiencies were obtained when Q_G/Q_L ratios and liquid flow rates are low and high respectively. On the contrary, from the 3-D "stool" shape obtained for the variation of liquid concentration, maximum liquid concentrations were obtained when Q_G/Q_L and Q_L are both high.

This study showed that BFCM is a simple, accurate and flexible modelling technique that can be applied to model ozone mass transfer in static mixers. The BFCM model will be further improved to include chemical reactions with particular emphasis on bromate formation and the extent to which ozone oxidation reactions develop.

References

[1] U.V. Gunten, Ozonation of drinkingwater: part II. Disinfection and by-product formation in presence of bromide, iodide or chlorine, Water Res. 37 (2003) 1469–1487.
[2] S.W. Krasner, W.H. Glaze, H.S. Weinberg, P.A. Daniel, I.N. Najim, Formation and control of bromate during ozonation of waters containing bromide, J. Am. Water Works Assoc. 85 (1993) 73–81.
[3] J.D. Plummer, J.K. Edzwald, Effect of ozone on disinfection by-product formation of algae, Water Sci. Technol. 37 (1998) 49–55.
[4] J.D. Plummer, J.K. Edzwald, Effect of ozone on algae as precursors for trihalomethane and haloacetic acid production, Environ. Sci. Technol. 35 (2001) 3661–3668.
[5] C. Traversay, R. Bonnard, C. Adrien, F. Luck, Static mixer: a reactor for the ozone process, in: IOA (Ed.), Fundamental and Engineering Concepts for Ozone Reactor Design, IOA, Toulouse, France, 2000, pp. 155–162.
[6] Q. Zhu, Ozone disinfection of sewage in a static mixer contacting reactor system on a plant scale, Ozone Sci. Eng. 13 (1990) 313–330.
[7] C.R. Schulz, P.W. Prendiville, Designing high concentration ozone contactors for drinking water treatment plants, Ozone Sci. Eng. 15 (1993) 245–266.
[8] Metcaf & Eddy, Wastewater engineering treatment and reuse, 4th ed., McGraw–Hill, New York, 2003.
[9] N. Martin, C. Galey, Use of static mixer for oxidation and disinfection by ozone, Ozone Sci. Eng. 16 (1994) 455–473.
[10] R.H. Bowman, HiPOx™ ozone-peroxide advanced oxidation system for treatment of trichloroethylene and perchloroethylene without forming bromate, in: IOA (Ed.), 16th Ozone World Congress, IOA, Las Vagas, USA, 2003, pp. 580–596.
[11] J. Leparc, C. Mysore, B. Marrino, L. Gurnari, Design of ozone and uv processes for drinking water disinfection based on pilot-scale studies, in: IOA (Ed.), 16th Ozone World Congress, IOA, Las Vegas, USA, 2003, pp. 739–761.
[12] P. Agutter, R. Lake, T. Burke, M. Chandrakanth, Full-scale comparison of the use of static mixers and diffusers for ozone injection, in: IOA (Ed.), 15th Ozone World Congress, IOA, London, UK, 2001, pp. 189–203.
[13] A.K. Bin, M. Roustan, Mass transfer in ozone reactors, in: IOA (Ed.), Fundamental and Engineering Concepts for Ozone Reactor Design, IOA, Toulouse, France, 2000, pp. 99–131.
[14] C. Mysore, J. Leparc, M. Prevost, J. Zuback, C. Owen, Selection of an ozone dissolution system for the Tampa Bay regional water treatment plant, in: IOA (Ed.), 16th Ozone World Congress, IOA, Las Vegas, USA, 2003, pp. 670–691.
[15] M. Chandrakanth, J. Leparc, R. Lake, Q. Agutter, Comparing static mixer performances at pilot- and full-scale for ozonation, inactivation of *Bacillus subtilis* and bromate formation in water treatment, in: IOA (Ed.), 15th Ozone World Congress, IOA, London, UK, 2001, pp. 24–35.
[16] Q. Zhu, C. Liu, Z. Xu, A study of contacting systems in water and wastewater disinfection by ozone. 2. Mathematical models of the ozone disinfection process with a static mixer, Ozone Sci. Eng. 11 (1989) 189–207.
[17] D.M. Hobbs, F.J. Muzzio, Reynolds number effects on laminar mixing in the Kenics static mixer, Chem. Eng. J. 70 (1998) 93–104.
[18] Z. Jaworski, P. Pianko-Oprych, Two-phase laminar flow simulations in a kenics static mixer—standard Eulerian and Lagrangian approaches, Chem. Eng. Res. Des. 80 (2002) 910–916.
[19] J.Z. Fang, D.J. Lee, Micromixing efficiency in static mixer, Chem. Eng. Sci. 56 (2001) 3797–3802.
[20] E.B. Nauman, D. Kothari, K.D.P. Nigam, Static mixers to promote axial mixing, Trans. IChemE A 80 (2002) 681–685.
[21] S.C. Jones, F. Sotiropoulos, A. Amirtharajah, Numerical modeling of helical static mixers for water treatment, J. Environ. Eng. ASCE 128 (2002) 431–440.
[22] M.H. Roemer, L.D. Durbin, Transient response and moments analysis of backflow cell model for flow systems with longitudinal mixing, Ind. Eng. Chem. Fundam. 6 (1967) 120–129.
[23] J. Zahradnik, M. Fialova, The effect of bubbling regime on gas and liquid phase mixing in bubble column reactors, Chem. Eng. Sci. 51 (1996) 2491–2500.
[24] W.J. Masschelein, Fundamental properties of ozone in relation to water sanitation and environmental applications, in: I.O. Association (Ed.), Fundamental and Engineering Concepts for Ozone Reactor design, International Ozone Association, Toulouse, France, 2000, pp. 1–30.
[25] J.A. Roth, D.E. Sullivan, Solubility of ozone in water, Ind. Eng. Chem. Fundam. 20 (1981) 137–140.
[26] S. Degaleesan, S. Roy, S.B. Kumar, M.P. Dudukovic, Liquid mixing based on convection and turbulent dispersion in bubble columns, Chem. Eng. Sci. 51 (1996) 1967–1976.
[27] A. Heyouni, M. Roustan, Z. Do-Quang, Hydrodynamics and mass transfer in gas–liquid flow through static mixers, Chem. Eng. Sci. 57 (2002) 3325–3333.
[28] W.H. Huang, C.Y. Chang, C.Y. Chiu, S.J. Lee, Y.H. Yu, H.T. Liou, Y. Ku, J.N. Chen, A refined model for ozone mass transfer in a bubble column, J. Environ. Sci. Health A 33 (1998) 441–460.
[29] C. Tizaoui, N.M. Grima, M.Z. Derdar, Effect of the radical scavenger *t*-butanol on gas–liquid mass transfer, Chem. Eng. Sci. 64 (2009) 4375–4382.